The Spacecraft Communications Blackout Problem Encountered during Passage or Entry of Planetary Atmospheres

D. D. Morabito[1]

During the Mars Pathfinder mission, there was a 30-second period in which the 8.4-GHz (X-band) communications link to Earth was lost during the atmospheric entry phase. An analysis of the Mars Pathfinder reconstructed flight profile using aero-thermodynamic tools provided estimates of the electron densities in the stagnation and wake regions of the spacecraft. For the wake region, where the low-gain antenna used to communicate with Earth was located, the electron-density estimates exceeded the critical X-band electron density during the first 20 seconds of the 30-second blackout period. High Doppler dynamics and low signal-to-noise ratio may have contributed to the blackout during the last 10 seconds. Thus, at least part of the Mars Pathfinder communications blackout during entry was possibly due to the sheath of charged particles generated by heating incurred by the shock. The upcoming Mars Exploration Rover (MER) missions, MER-A and MER-B, scheduled for 2003 launches, are not expected to experience communication blackouts due to charged particles during their entry phases into the Martian atmosphere in 2004. The estimated peak electron densities expected for MER lie about three orders of magnitude below the critical X-band electron density required for blackout.

I. Introduction

Several missions have flown or are being planned to fly in which space probes will descend into planetary atmospheres to realize a variety of objectives. Such missions include landers, rovers, and airplanes, as well as orbiting spacecraft, which will use the planetary atmosphere to slow them down and enable aerocapture in order to save fuel to bring them into orbit. When a spacecraft enters a planetary atmosphere at a velocity significantly exceeding the speed of sound, a shock layer forms in front of the body. The sheath of ionized particles, which develops around the spacecraft, is the result of ionization of the atmospheric gases as they are compressed and heated by the shock, or heated within the adjacent boundary layer. When the electron density gets sufficiently high, such that it exceeds the critical plasma density of the link frequency, communications can be disrupted, with the result being significant attenuation or even blackout. The main cause of blackout is reflection or absorption of electromagnetic energy at frequencies

[1] Communications Systems and Research Section.

The research described in this publication was carried out by the Jet Propulsion Laboratory, California Institute of Technology, under a contract with the National Aeronautics and Space Administration.

below the critical plasma frequency. At frequencies higher than the plasma frequency, the layer will be effectively transparent to the transmitted signal, and communications can take place.

In order to assess any potential blackout problem, the velocity and altitude flight profile during passage through the planetary atmosphere can be analyzed by using aero-thermodynamic tools. Such programs make use of planetary atmospheric information such as composition, pressure, temperature, and density. Other information used as input to these programs includes heat of formation and molecular weight of each species, which are initially present or are the result of heating with the initial atmosphere. The free energies and enthalpies as a function of temperature for each species are also input in the calculations.

The output of such programs includes the velocity of the shock layer and the densities of all of the chemical species that may be present, including electron density at the stagnation point. The electron density is the result of the combined concentrations of the various ionized species, which are generated due to the high temperatures encountered. Since antennas used for communication during atmospheric passage are mounted on the back shell of the spacecraft (such as that for Mars Pathfinder), the electron density in the wake region is estimated from the stagnation electron density, using appropriate approximations. The wake-region density will be significantly less than the stagnation point density, but still could exceed the critical blackout electron density in some cases.

During the descent of the Mars Pathfinder spacecraft into in the Martian atmosphere on July 4, 1997, communications with Earth were lost for an approximately 30-second period starting at about 17:03:20 UTC [1]. The emitted signal frequency of 8.43 GHz was received in the one-way tracking mode at the NASA Deep Space Network (DSN) 70-m antenna located in Madrid, Spain. Among the several possible explanations for the outage was one that attributed it to ions generated from the interaction of the heat shield with the atmosphere. To test the likelihood of this possibility, the flight profile of Pathfinder during the blackout period was input to an aero-thermodynamic program to estimate electron density. The electron-density results output from the aero-thermodynamic program, developed by T. Horton at JPL [2], did exceed the critical electron density required for blackout at 8.4 GHz (X-band), at least during the first 20 seconds of the blackout period.

Such aero-thermodynamic tools also can be used to predict whether blackout conditions might occur for upcoming missions, such as the Mars Exploration Rover (MER) entry at Mars or a proposed aero-capture demonstration experiment during atmospheric passage with Earth.

Earlier work on communications blackout at Mars included that of Nordgard [3], who made predictions for several flight profiles of blunt body capsules entering the Martian atmosphere. For the trajectories considered, Nordgard concluded that a blackout condition would easily occur at a frequency of 2.3 GHz (S-band). Nordgard also performed a detailed study of atmospheric reflection and refraction of the telemetry signals near a blackout condition. Other early studies of the Martian atmosphere effect on entry vehicle communications included the work of Dwain Spencer in 1964 [4], who used the JPL program [2] to obtain equations of electron density as a function of flight profile points of velocity and atmospheric density.

The space vehicles of Projects Mercury, Gemini, and Apollo experienced significant several-minute-long communication blackouts during their atmospheric re-entry phase. In the 1960s, NASA conducted several experiments involving Earth atmospheric re-entry. Brummer [5] proposed the use of an X-band telemetry system to alleviate the radio blackout problem for Earth re-entry vehicles over lower frequency bands, which, for instance, resulted in an agonizing 4-minute blackout period for Project Mercury. For Apollo, the interaction of the high-speed blunt capsule with the Earth's atmosphere caused communication blackouts of from 4 to 10 minutes in duration at S-band. Dunn [6] compared predicted and measured communication blackout boundaries of atmospheric-density and velocity profiles for Apollo. The Horton program was used to estimate the charged-particle densities at the Apollo S-band blackout boundaries, which were then compared with the critical S-band electron density. The Horton program also was run using the flight profile of a proposed Earth aero-capture demonstration to estimate electron density, which was then compared with the critical electron density for several possible link frequencies.

In addition to the Horton program, the Langley Aero-Thermodynamic Upwind Relaxation Algorithm (LAURA) program provided spot checks of the Horton program results. The LAURA program was run using the chemical kinetic and thermal non-equilibrium two-temperature model of Park et al. [7]. This model also included 18 species and 3 momentum and 2 energy equations resulting in 23 simultaneously solved equations at each computational data point. Detailed descriptions of conservation equations and physical models used by the LAURA program are provided in [8]. Comparisons of LAURA estimates to experimental data have been well documented in the literature [9, references therein].

II. Effects of Charged Particles on Communications

The surrounding plasma on a spacecraft entering a planetary atmosphere will attenuate any radiated signal by absorption and reflection if its density is sufficiently high. Electrons are the main contributors to reflection of waves in a plasma gas [4]. The propagation condition normally will depend on the transmission frequency, the electron collision frequency, and the plasma frequency of the charged-particle sheath. The electron collision frequency is the number of collisions per second that the electrons encounter with other species in the plasma, and this normally would determine the degree of attenuation when the transmission frequency is exceeds the plasma frequency [4]. Since the collision frequency usually is much smaller than the critical plasma frequency, the collision effects on wave propagation normally are not considered important for communications, although they are important for determining the thermodynamic state of the gas [4].

The propagation constant can be represented as a complex number, and the extinction coefficient can be shown to be [4]

$$k' = \sqrt{\frac{f_p^2 - f^2}{f^2}} \tag{1}$$

where f_p is the plasma frequency and f is the frequency of interest.

The effect of charged particles generated by the heating of atmospheric gases or by an ablating heat shield as a spacecraft enters an atmosphere will be to black out the signal if the resulting charged-particle density exceeds the plasma density at that frequency. For a given electron density (also understood to be electron number density), the plasma frequency, in Hz, is expressed as

$$f_p = \frac{1}{2\pi}\sqrt{\frac{q^2 n_e}{\varepsilon_0 m_e}} \tag{2}$$

where

$q =$ electron charge, 1.6×10^{-19} coulombs

$n_e =$ electron number density per cubic meter, m^{-3}

$m_e =$ electron mass, 9.1×10^{-31} kg

$\varepsilon_0 =$ permittivity, 8.85×10^{-12} $\mathrm{F/m}^2$

The signal will be attenuated for frequencies that fall below the plasma frequency and will be unaffected for frequencies that lie above the critical plasma frequency. There will be some attenuation for $f > f_p$, but this usually is considered negligible.

Conversely, given a communications link frequency, f_{link} in Hz, the critical electron density can be found for which communications will be disrupted when that critical density is exceeded, and communications will be nominal when the electron density lies below that critical density. Rewriting Eq. (2) in terms of $n_{e,crit}$ (now in units of cm^{-3}), we have

$$n_{e,crit} = \frac{f_{\text{link}}^2}{80.64 \cdot 10^6} \tag{3}$$

The critical plasma densities estimated from Eq. (3) for a few well-known link frequencies are given in Table 1. The critical density is expressed in particles/cm^3, a commonly used density unit.

The total attenuation per unit length can be expressed as [4]

$$\frac{\text{dB}}{z_p} = \frac{54.6}{\lambda} k' \tag{4}$$

where k' is as given in Eq. (1) and λ is the wavelength of the radio wave. This amount of attenuation per unit length as a function of electron density is plotted in Fig. 1 for the several common downlink frequencies used for "proximity" link and deep-space communications. As the critical density is reached and exceeded, the attenuation per unit length increases rapidly, such that a communications blackout is

Table 1. Critical electron densities.

Link frequency, GHz	Designation	Critical electron density, particles/cm^3
0.401	UHF	1.99×10^9
2.3	S-band	6.56×10^{10}
8.4	X-band	8.75×10^{11}
32.0	Ka-band	1.27×10^{13}

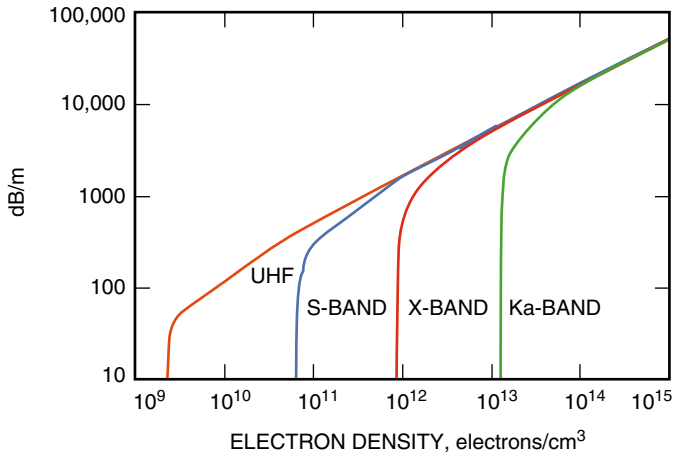

Fig. 1. Attenuation per unit length versus electron density.

in effect for nominal signal-to-noise ratios (SNRs), given that a typical plasma thickness from a fore-body wall can range from a few to tens of centimeters. The typical approach during atmospheric entry is to maintain carrier visibility as long as possible and to simplify operations as much as possible. Thus, frequency semaphores may be used to relay spacecraft conditions. Telemetry is recorded onboard during the expected blackout period and transmitted when communications are later restored. The use of higher frequencies can reduce the blackout period or eliminate the blackout condition entirely.

III. The Use of Aero-Thermodynamic Modeling to Predict Electron Density

Aero-thermodynamic tools have been used in a wide variety of applications for several different atmospheric flight applications and scenarios. These include entry vehicles and spacecraft as they fly through a gaseous environment such as a planetary atmosphere. These tools have been used to investigate aero-thermodynamic problems of normal shock, flow field, convective heat transfer, and radiative heat transfer, as well as communications blackout. Such a program is the JPL Normal Shock and Chemical Equilibrium Program, which was developed and first used in the 1960s [2]. This program calculates chemical equilibrium properties associated with traveling, standing, and reflected normal shocks.

The JPL Horton program [2] was originally programmed in FORTRAN II for use on IBM 7090 or 7094 computers. The program code was recovered from the listing provided in [2] and modified into modern-day FORTRAN 77 for use on a Sun SPARC [tm] 5 workstation under the Sun Solaris [tm] operating system. Appropriate modifications were made to the code, replacing obsolete input/output devices with modern-day input/output interfaces and accommodating currently used conventional units, such as km/s for velocity (versus ft/s). In the 1960s, the computer required 15 seconds to execute each normal-shock solution [2]. Today, the computer takes less than 0.01 seconds to execute a program run of 203 consecutive normal-shock solutions.

The library data file required by the Horton program as general input was also recovered from the partial listing in [2], the references listed in [2], and data obtained from references published since the 1960s. The input files used by the program for three test cases also were recovered from [2]: Case 1—Mollier data, Case 2—normal shock problem (Mars atmosphere), and Case 3—combination normal shock (Earth atmosphere). The recovered Horton program was run using the test cases as input, and the program was debugged until agreement was achieved by comparing the program output listings with the test-case output listings provided in [2].

The program was run for specific Mars and Earth atmosphere entry flight profile cases. The Mars-entry cases included the Mars Pathfinder reconstructed entry profile and the MER predicted entry profile. The Earth-entry cases included the profile of Apollo mission blackout boundaries and a flight profile of a proposed Earth atmospheric aero-capture demonstration.

The following program description closely follows the text and terminology provided by Horton [2]. The program accommodates up to 36 ($s = 36$) different compounds (CN, NO^+, CO, NO, NO_2, N_2O, CO_2, N_2, O_2, C^{+++}, C^{++}, C^+, C^-, CO^+, C_2N_2, C_2, C_3, N^{+++}, N^{++}, N^+, N_2^+, O^{+++}, O^{++}, O^+, O^-, O_2^-, O_2^+, O_3, Ar^{+++}, Ar^{++}, Ar^+, C, N, O, e^-, Ar), which are combinations of 5 ($m = 5$) different elements (C,O,N,Ar,e^-), where free electrons (e^-) are treated as an element. The program considers dissociation and ionization effects for temperatures between 1000 K and 20,000 K. The general library file input consists of the formula vector, heat of formation and molecular weight for each of the 36 species, and arrays of free energy and enthalpy versus temperature (1000 K to 20,000 K in steps of 500 K) for each species. The program input for each case includes the initial neutral gas mixture of the planetary atmosphere and the initial pressure and temperature of the mixture. The program output includes a chemical description of the gas, including the electron number density.

The foundation for determining the chemical equilibrium properties of a system, including its composition, follows from two important concepts: (1) the principle of conservation of mass of an elemental

species and (2) the second law of thermodynamics [2].[2] It is assumed that the time for a process to accommodate itself to local conditions within a region is very short compared to the transit time across this region. This implies that the mixture is in a state of equilibrium and allows for the behavior of each constituent to be described by the ideal gas equation. Given that m chemical elements combine to form s compounds, the assumption of a constant mass system in mechanical and thermal equilibrium at temperature T and pressure P requires the chemical composition to be such that the Gibbs[3] free energy is a minimum [2].

The Gibbs free energy, F, can be thought of as the chemical reaction potential energy of a substance or system, used to determine if a specific chemical reaction will spontaneously occur or not. The Gibbs free energy is expressed as

$$F = H - TS$$

where

$H =$ enthalpy (energy contribution due to motion of particles)

$T =$ absolute temperature

$S =$ entropy, or degree of disorder of a system

Thus, the free energy of the mixture can be related to quantities of the individual constituents and system by [2]

$$\frac{F}{RT} = \sum_{i=1}^{s+m} N_i \left(\frac{f_i^\circ}{RT} + \ln P + \ln \frac{N_i}{N} \right) \tag{5}$$

where the requirement that the free energy be a minimum is expressed as [2]

$$\frac{d}{dN_i} \left(\frac{F}{RT} \right) = 0 \tag{6}$$

where f_i° is the partial molal free energy of the ith constituent at one atmosphere, at temperature T, and is a function of $h_{0,i}^\circ$, the molal heat of formation of the ith constituent at 0 K and one atmosphere. It is also a function of the specific heat at constant pressure $C_{P,i}$ and at temperature T, and where

$R =$ ideal gas constant, 8.31 J/K-mole

$T =$ temperature, K

$P_i =$ pressure of the ith constituent, atm

$N_i =$ number of particles of the ith constituent

$N =$ total number of particles in the system

Thus, using Eqs. (6) and (5), the system of equations becomes [2]

[2] The second law states that entropy in the universe is increasing.

[3] Josiah Willard Gibbs (1839–1903) is considered one of the great American scientists of the 19th century. He received the first Doctor of Engineering in the United States.

$$0 = \sum_{i=1}^{s+m} \left(\frac{f_i^\circ}{RT} + \ln P + \ln \frac{N_i}{N} \right) dN_i \tag{7}$$

The constraint of conservation of mass of the chemical elements requires that [2]

$$0 = dN_j + \sum_{i=1}^{s} \alpha_{ij} dN_i$$

where $j = s+1, s+2, \cdots, s+m$ and α_{ij} is the formula vector that indicates the number of atoms of the jth numbered element for the ith numbered compound or ion.

The constraint equations are then combined, which results in elimination and simplification of terms. The concentrations of each of the s species, $dN_i, i = 1, \cdots, s$, are assumed to be independent. Further manipulation results in the equations of mass action and mass balance. Linearized forms of these equations are obtained using series expansions with temperature, density, and initial molal concentrations. The linear system of $s+m$ equations is simplified to m equations, after elimination of some parameters. Initial values for the concentrations are input to the system of equations at a selected temperature, density, and concentration under standard conditions, and the coefficients are then evaluated. The solution to the system is found using the Crout method [2], and the new values of concentrations are obtained from the equation of mass action, which replaces the initial or previous values. The procedure is repeated until the difference of the $(k+1)$ and k iteration estimates of the mixture concentration, mixture density, and enthalpy per unit volume satisfy a convergence criterion. Once the convergence criterion is satisfied, the result is a set of concentrations at the $(k+1)$ iteration of each species that agrees with the k iteration values.

The focus from this point onward is consideration of the free-flight or moving shock problem, which is the case of interest for the atmospheric entry blackout problem, such as for Mars Pathfinder entering into the Mars atmosphere at an atmospheric relative velocity of v_F (see Fig. 2). The coordinate system is specified such that flow is steady and one-dimensional in the x direction. The effects of body forces, diffusion, and radiative transfer are considered negligible. The equations of continuity, linear momentum, and energy are integrated with respect to x and are applied across a normal shock. If either (1) the fluid is inviscid (having zero viscosity) and non-heating or (2) the fluid is in thermodynamic equilibrium, these equations relating the thermodynamic properties and velocities upstream in region A and downstream in region B of a flow field associated with the normal shock will thus reduce in form [2]:

$$\rho_A v_A = \rho_B v_B \tag{8}$$

$$\rho_A v_A^2 + P_A = \rho_B v_B^2 + P_B \tag{9}$$

$$H_A + \frac{v_A^2}{2} = H_B + \frac{v_B^2}{2} \tag{10}$$

The properties behind the bow shock associated with a high-velocity blunt body that is propagating in a quiescent gas at a specific velocity are determined using the Hugoniot equation, which is derived from Eqs. (8) through (10) [2]:

$$H_G - H_\infty = \frac{1}{2} \left(P_G - P_\infty \right) \left(\frac{1}{\rho_\infty} + \frac{1}{\rho_G} \right) \tag{11}$$

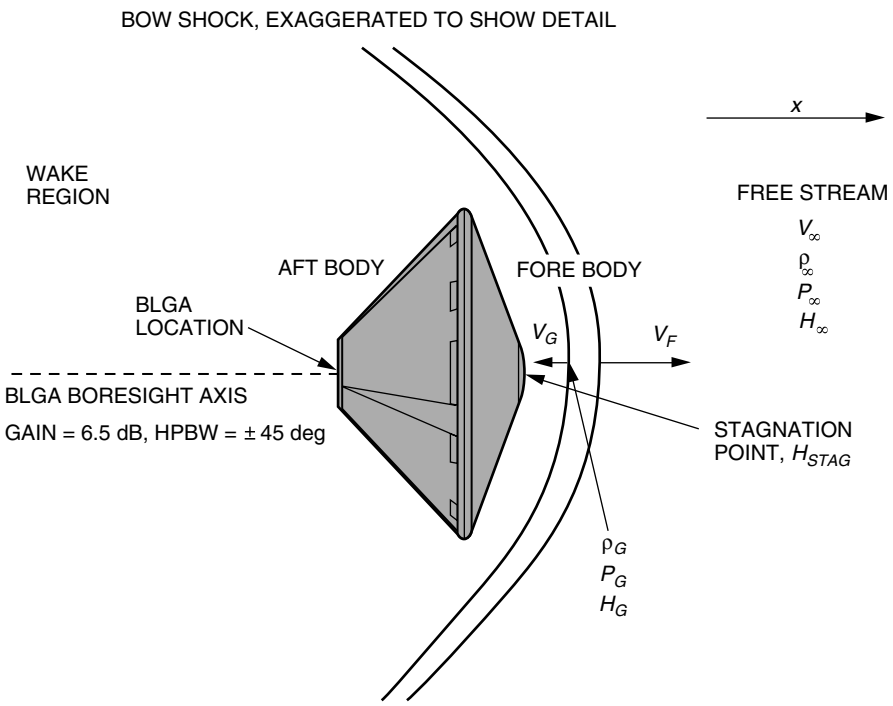

Fig. 2. Mars Pathfinder atmospheric entry scenario.

The moving shock problem is used to find a thermodynamic state, defined by the temperature and density, that satisfies the Hugoniot equation at the given initial conditions of pressure, temperature, and density [2]. The temperature and density are varied until values of pressure and enthalpy are obtained that satisfy Eq. (11). Because the enthalpy H and pressure P are functions of density and temperature, the selection of properties in one region will allow the properties in the other region to be obtained using Eq. (11).

The iterative procedure used to find the correct value of density is the Newton–Raphson method [2] using an expanded version of the Hugoniot equation. The procedure is iterated until agreement is reached, such that the new and previous estimates agree based on the convergence criteria [2]. The flight velocity (or shock velocity) is expressed by [2]

$$v_F = \sqrt{\frac{\rho_G}{\rho_\infty}\left(\frac{P_G - P_\infty}{\rho_G - \rho_\infty}\right)} \tag{12}$$

The velocity of the gas behind the shock, relative to the spacecraft, is given by [2] (see Fig. 2):

$$v_G = \sqrt{\frac{\rho_\infty}{\rho_G}\left(\frac{P_G - P_\infty}{\rho_G - \rho_\infty}\right)} \tag{13}$$

The enthalpy at the stagnation point is given by [2] (see Fig. 2):

$$H_{STAG} = H_G + \frac{1}{2}v_G^2 \tag{14}$$

Once properties are found that satisfy Eq. (11), Eq. (12) through (14) are evaluated [2]. These equations approximate free-flight conditions for the case when the gas is in chemical equilibrium. The effect of wall shear and heat transfer are considered negligible. The shape of the vehicle is not modeled in the calculations. The use of this method will start to break down at higher altitudes or under conditions such that the gas is in a state of non-equilibrium.

IV. Approach for Estimating Electron Density during Planetary Atmospheric Entry

In order to estimate the density of electrons in the region around a spacecraft entering a planetary atmosphere using the Horton program, a flight profile consisting of a series of atmosphere-relative velocity and altitude time-tagged points is required. When actual reconstructed atmospheric density as a function of flight altitude is available, such as was the case for Mars Pathfinder in [10], it can be input directly into the program (after appropriate normalization).

If the reconstructed atmospheric density or pressure profiles are not available, such as for proposed or upcoming flights, the atmospheric pressure, P, as a function of altitude, h, can be approximated by

$$P = P_S \exp\left(\frac{-h}{H}\right) \tag{15}$$

where P_s is the surface pressure and H is the scale height of the atmosphere. Nominal values of these parameters are given in Table 2 for Earth and Mars. Surface pressure and scale heights can vary depending upon assumed conditions and altitude range. Variations of this formula can be used that involve different temperature dependencies for different layers of the atmosphere, such as the upper and lower stratospheres. The Horton program accepts normalized pressure $P/P_{S,\mathrm{Earth}}(P/1013)$ as an input parameter.

A series of normal shock cases using the Horton program at a given input pressure are run for several different "expected" shock temperatures. The program output includes values of shock velocity and electron density for each case. The electron density is referred to the stagnation point, which lies near the nose on the fore-body of the vehicle encountering the shock as the vehicle transits the atmosphere (see Fig. 2). This estimate is obtained from the normal shock solution for the temperature, which produces the shock (or free-flight) velocity [Eq. (12)] closest in agreement with flight-path profile velocity for that point. In some cases, non-linear interpolation is performed over several solution pairs of electron density and shock velocity to reference the curve at the actual flight profile velocity in order to yield a better estimate of electron density.

Since the antenna used for communications with Earth usually lies in the rear of the vehicle, such as for Mars Pathfinder, it is desirable to estimate the electron number density in the wake region (see

Table 2. Nominal atmospheric parameters.

Planet	Surface pressure, mbar	Scale height, km	Isentropic expansion coefficient
Earth	1013	7	1.4
Mars	6.1	11.1	1.33

Fig. 2). The ratio of electron number density in the wake region to that at the stagnation point can be estimated using [4]

$$\frac{n_{e,w}}{n_{e,s}} = \left[\frac{\kappa P_\infty}{P_G}\right]^{1/\gamma} \tag{16}$$

where P_∞/P_G is the pressure ratio across the shock region (an output of the program for the given flight-profile point), γ is the isentropic expansion coefficient (or ratio of specific heats), which ranges from 1.3 to 1.4 (see Table 2), and κ is a correction factor normally taken to be unity. For this study, a value of $\gamma = 1.33$ was adopted for Mars,[4] and $\gamma = 1.4$ for Earth. The approximation of Eq. (16) can produce different results because the expansion coefficient, γ, is not constant as the gases expand, and the wake-region pressure can be significantly higher than the free-stream pressure, P_∞, during certain stages of the atmospheric entry profile. Thus, the inclusion of the factor κ in Eq. (16) will allow for a better approximation of the wake-region electron number concentration.

The wake-region electron number density using Eq. (16) is then compared with the critical electron number density at the link frequency (Table 1) to determine if a communications blackout condition is likely. This assumes that the communications antenna is located in the wake region. Using this frozen-flow approximation, the electron density in the stagnation region is assumed to remain constant as the gases flow around the spacecraft into the wake region. The approximation does not account for any recombination, and the change in density is due entirely to the expansion of the gases. This method is thus considered conservative [4] and can usually serve as an upper bound on the wake-region electron density. The uncertainty on the electron number density estimates is believed to be about an order of magnitude. The program estimates of electron number density were found to be in agreement with independently determined values to the ∼50 percent level (see Sections VI.C and VII). Thus, the basic rule of thumb for testing for a blackout condition is (1) if the calculated electron number density lies below the critical plasma number density by more than an order of magnitude, blackout is deemed unlikely, (2) if the calculated electron density lies above the critical electron number density by more than an order of magnitude, blackout is deemed likely, and (3) if the calculated electron number density is within an order of magnitude of the critical number density, blackout is deemed uncertain, but possible.

V. Mars Atmosphere Models

The composition of the atmosphere of the planet Mars was not known very well in the earlier decades of space exploration. The main constituents of the atmosphere were assumed to be nitrogen, argon, and carbon dioxide, but the relative proportions were not well known. The early Mars atmosphere model used by Spencer [4] to make preliminary estimates of the stagnation and wake electron densities for an incoming vehicle assumed 30 percent CO_2, 40 percent N_2, and 30 percent argon, with an overall surface pressure of 11 mb. Spencer ran the Horton program using this 1960s Martian atmosphere model as input for different velocity and density values and performed empirical fits to the output charged-particle concentration estimates. From these runs, Spencer fitted equations of the form [4]

$$F = c\rho^a V^b \tag{17}$$

for both the stagnation and wake-region electron densities (in number/cm^3), where V is the atmospheric relative velocity in km/s and ρ is the free-stream atmospheric density in gm/cm^3 at the trajectory point of interest.

[4] C. Ho, personal communication, Jet Propulsion Laboratory, Pasadena, California, April 2002.

Spencer's fit values were within 50 percent of the calculated values for a range of shock velocities between 4.3 km/s and 9.1 km/s. The fit was biased to produce a conservative result for velocities above 6.7 km/s. For the 1960s Mars atmosphere model, the Spencer fit of stagnation electron density versus velocity and density in Eq. (17), took the form [4]

$$N_{e,s} = 1.5 \times 10^{10} \rho^{0.95} V^{11.8} \quad \text{(stagnation)} \tag{18}$$

Spencer described different methods for estimating the wake-region electron density where an antenna was likely to be located for direct communications with Earth. The frozen-flow assumption of Eq. (16) was used to estimate the wake-region electron densities from the stagnation densities. Spencer fit the wake-region densities with Eq. (17) to get [4]

$$N_{e,w} = 1.83 \times 10^{9} \rho^{0.95} V^{10.37} \quad \text{(wake region)} \tag{19}$$

A deficiency of the 1960s Marian atmosphere model is that the relative proportions of the constituents are significantly in error. A Martian entry propagation study conducted by Nordgard [3] made predictions of electron density. Although the composition of the Martian atmosphere was still not yet well known in 1976, Nordgard [3] did consider two models, which contained higher proportions of CO_2 (70 percent and 100 percent).

The modern day Martian atmosphere model assumes a surface pressure of about 6.1 mb and proportions of 95.3 percent CO_2, 2.7 percent N_2, and 1.6 percent argon. An argon-free simplification Martian atmosphere model is also considered as it was used as input to the Horton program to facilitate comparisons with the Langley Research Center LAURA program results, which neglects argon because it does not contribute much to the overall production of free electrons during atmospheric entry. Table 3 lists the model atmospheres that were considered for Mars.

Table 3. Martian atmosphere models considered.

Model	P_s, mb	CO_2, percent	N_2, percent	Argon, percent
Old 1960s	11	30	40	30
Modern day	6.1	95.3	2.7	1.6
Modern, no argon simplification	6.1	96.5	3.5	0

VI. Mars Pathfinder Atmospheric Entry

Mars Pathfinder entered the atmosphere of Mars on July 4, 1997, with an inertial velocity of 7.26 km/s directly from an interplanetary trajectory. The aero-shell consisted of a fore-body heat shield and an aft-body back shell (see Fig. 2). The aero-shell diameter was 2.65 m, and the fore-body shape was a 70-deg half-angle spherical cone with a nose radius of 0.6638 m and a shoulder radius of 0.0662 m [10]. The spacecraft used a back-shell low-gain antenna (BLGA) to communicate with Earth. The fore-body ablative material was SLA-561V, with a thickness of 19.05 mm. The back shell was thermally protected using a spray-on version of the SLA-561 material. [10].

The spacecraft reached maximum stagnation point heating and peak dynamic pressure within the first 80 seconds of the entry phase. Atmospheric entry is defined as the point at which the probe reaches an

altitude of about 125 km above the surface. The maximum heating rate occurred at 75 seconds past entry, and maximum dynamic pressure occurred near 78 seconds past entry, when the acceleration was 15.9 g's. Peak heating occurred at 68 seconds past entry, as determined from trajectory and reconstructed atmospheric information [10].

During the descent of Mars Pathfinder into the Martian atmosphere on July 4, 1997, communications with Earth were lost for an approximate 30-second period from 17:03:18 UTC to 17:03:49 UTC.[5] The reconstructed flight-path profile of Spencer et al. [10] specified that the parachute deployment occurred at 170 seconds past entry. Using the Wood et al. [1] time references of parachute deployment at 17:05:21 UTC and loss of signal (LOS) at 17:03:20 UTC, the blackout began at 49 seconds past entry, using the time past entry definition of Spencer et al. [10]. The blackout occurred while the spacecraft was in the continuum regime of the atmosphere. The expected transmitted signal at a frequency of 8.43 GHz was recorded at the NASA DSN 70-m antenna located in Madrid, Spain. Several possible explanations for the communications outage were provided by [1]. One explanation provided in [1] implied the loss of communication was due to ions created from the interaction of the heat shield with the atmosphere.

The Mars Pathfinder BLGA antenna used during the atmospheric entry phase, which included the blackout period, is of a circular waveguide three-ring choke design.[6] The BLGA has a gain of 6.5 dB on axis and an omni-directional antenna pattern with a half-power beamwidth of ± 45 deg. The BLGA is made of beryllium copper and is located on the back shell of the spacecraft (see Fig. 2). The bore of the BLGA has a shuttle tile plug mounted in the circular waveguide choke, with a thin ceramic coating on the top since the shuttle tile is porous. The material surrounding the choke is made up of circa material.

A. Old Mars Atmosphere Model Case

The flight profile used for the Mars Pathfinder entry was obtained from figures published in [10]. These figures consisted of atmospheric relative velocity versus time past entry, altitude above landing site versus time past entry, and altitude versus atmospheric density. The atmosphere relative velocity versus time of Mars Pathfinder is shown in Fig. 3(a). The altitude versus time of entry profile is shown in Fig. 3(b). The reconstructed Martian atmosphere using Mars Pathfinder data of neutral atmospheric density and velocity profile provided in [10] allowed for estimates of electron densities in the stagnation and wake regions using Eqs. (18) and (19), based on Spencer's fits for shock velocities ranging between 4 and 9 km/s [4].

Figure 4 displays the profiles of these two electron-density signatures (stagnation and wake) using reconstructed density and velocity data from [10] as input to the Spencer equations [4]. Although the stagnation curve lies above critical X-band plasma electron density, the wake-region curve (where the communication antenna is located) lies below critical X-band plasma electron density. From this result, one would conclude that Mars Pathfinder would not likely suffer a blackout, given that the antenna was transmitting out of the wake region. However, the wake-region curve's peak plateau is very well aligned with the known Pathfinder blackout period, depicted by the heavy black bar in Fig. 4. Thus, both stagnation and wake-region curve peaks align with the known Mars Pathfinder blackout period.

However, the Mars atmosphere model used was outdated and has since been revised. Spencer [4] cautioned that doubling the amount of CO_2 in the atmosphere will double the electron density because carbon is the principal contributor of electrons. The known Mars atmosphere has a factor of 3.2 increase of CO_2 over that in the old Mars atmosphere model (see Table 3). Thus, a significant increase in the electron density during the Pathfinder descent is expected due to the increased amount of CO_2 in the Mars atmosphere model that is accepted today.

---

[5] E. Satorius, *Mars Exploration Rover X-Band EDL Peer Review,* internal document, Jet Propulsion Laboratory, Pasadena, California, June 11, 2002.

[6] J. Vacchione, personal communication, Jet Propulsion Laboratory, Pasadena, California, November 19, 2001.

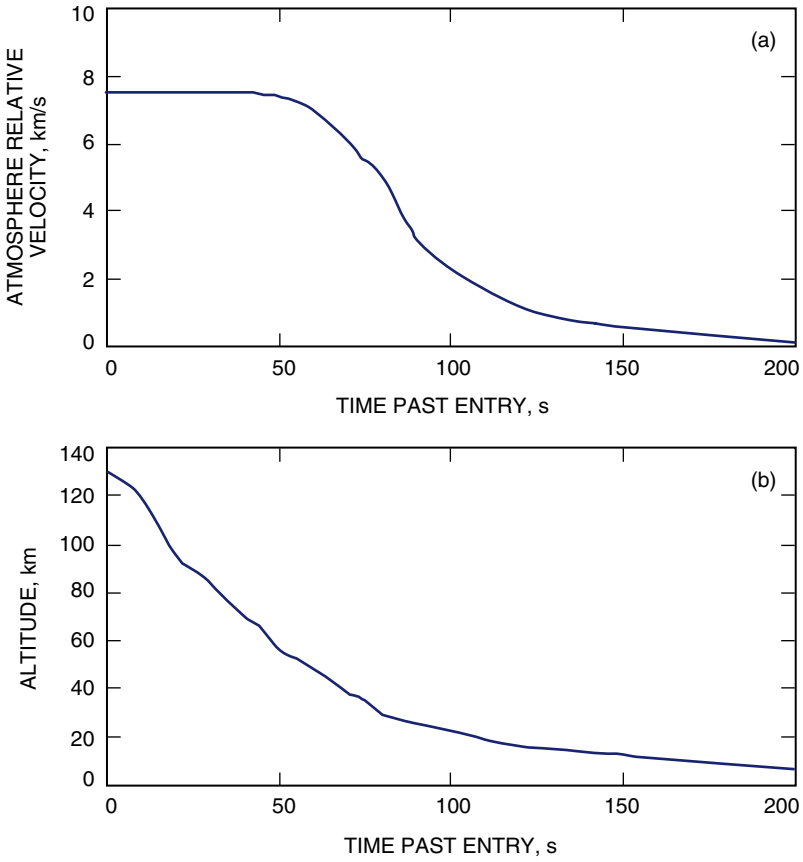

Fig. 3. Mars Pathfinder (a) atmosphere relative velocity versus time past entry and (b) altitude versus time past entry.

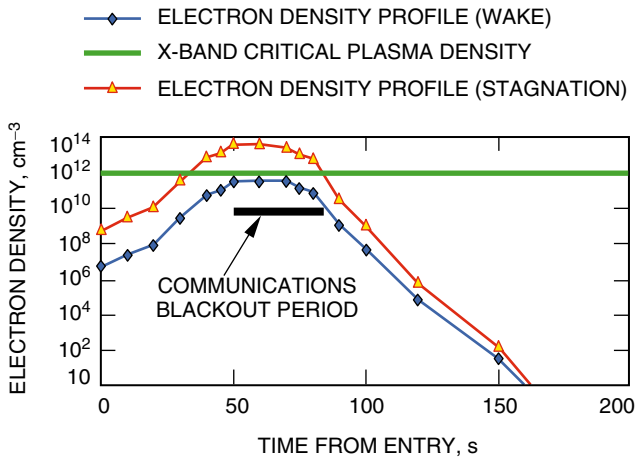

Fig. 4. Mars Pathfinder old Mars atmosphere model.

Given that the atmospheric model used to generate the curves of Fig. 4 was based on an outdated 1960s Mars atmosphere model, and that a communications blackout did occur, it was realized that the electron densities needed to be re-estimated using the current-day Mars atmosphere model in order to learn whether or not the communications blackout could possibly have been caused by the sheath of charged particles generated by shock heating during the atmospheric entry of Mars Pathfinder.

B. Revised Mars Atmosphere Case

The Horton program was run using the current-day Mars atmosphere model with no argon simplification (see Table 3) for several entry flight-path trajectory points, which include the blackout period (Fig. 5), from [10]. These estimates were obtained using the approach given in Section IV. The "no-argon simplification" was used as input to the Horton program to facilitate comparisons with the Langley Research Center LAURA program (see Subsection VI.C), which used a no-argon atmospheric model since argon is not expected to contribute significantly to the generation of electrons. The wake-region electron number density was approximated from the stagnation point number densities and pressure ratios output from the Horton program, using values of $\gamma = 1.33$ and $\kappa = 3.5$ in Eq. (16). The free stream-to-wake region pressure correction factor, κ, was estimated from a set of stagnation and wake-region number densities output from the LAURA program.

Note that in Fig. 5 the wake-region electron number density curve does lie above the critical electron number density for the first 20 seconds, coinciding with the start of the observed blackout period. This supports the hypothesis that at least the first 20 seconds of the Mars Pathfinder communications blackout possibly was due to a sheath of charged particles created by shock-induced thermal heating and compression of atmospheric gases. Given that the resulting electron number density estimates are within an order of magnitude of the critical plasma number density for X-band during the blackout period, and that the expected uncertainty is of an order of magnitude, caution must be exercised in interpreting this result.

The first 20 seconds of the Mars Pathfinder blackout period are consistent with loss of signal due to the high density of charged particles forming about the spacecraft (see Fig. 5). For flight-profile points during this period, the wake-region electron-density estimates exceed the critical electron density necessary for blackout at X-band. Independent checks for flight-profile points during this blackout period at 50 seconds and 60 seconds past entry, using the Langley LAURA program, support this result (see Subsection VI.C).

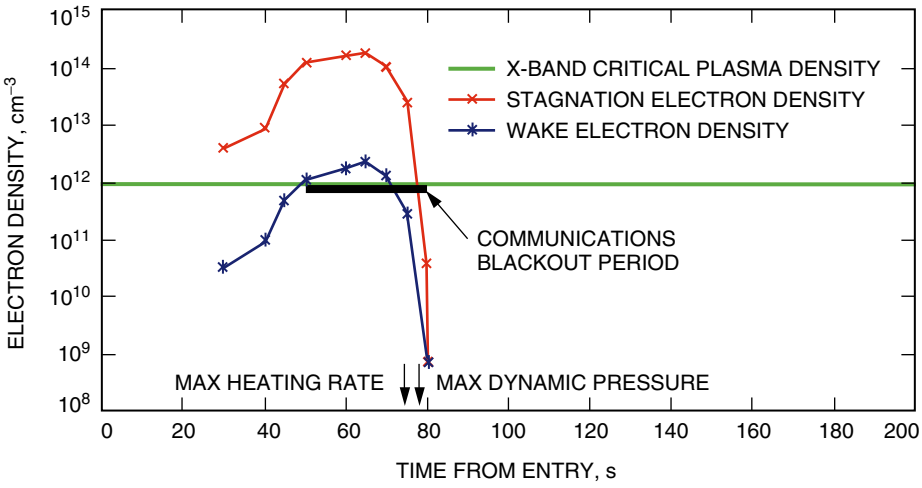

Fig. 5. Mars Pathfinder new Mars atmosphere model, no argon.

Post-experiment spectral analyses of the received carrier signal just before blackout revealed broadening of the signal spectrum [1],[7] which provides supporting evidence that charged particles may have contributed to the blackout.

During the last 10 seconds of the observed blackout period, the predicted wake-region number densities computed by both the Horton program and the LAURA program fall below the critical X-band electron number density. The continuation of the blackout period during this time could be attributed to complications caused by a combination of other factors, including high Doppler dynamics and any attenuation, reflection, or spectral broadening effects from the remaining charged particles, which could have lowered the received SNR just below threshold or induced impedance mismatch effects on the antenna.

The carrier signal initially present in the open-loop receiver bandpass was found to have been replaced by the subcarrier when the signal was reacquired at the end of the blackout period [1]. A few seconds later, the carrier then returned in the receiver bandpass, replacing the subcarrier [1]. The SNR of the signal was only 4 dB when it was detected just after coming out of the blackout period, based on the fast Fourier transform (FFT) analysis performed on the open-loop data [1]. Given that the SNR was very low, the signal could have been lost due to additional attenuation attributed to other factors, such as the finite electron collision frequency, even though the link frequency exceeded the estimated plasma frequency during this period. Based on estimates of electron collision frequencies at low altitudes (about 30 km), estimates of attenuation were found to be small [4]. Although the blackout region is not expected to extend to lower altitudes when collisions are included, this study should be revisited using modern-day chemistry advances and aero-thermodynamic tools in light of the Mars Pathfinder result.

C. Comparisons with Langley LAURA Program

The LAURA program employs upwind-biased point implicit relaxation and is sufficiently robust to achieve convergence at near-equilibrium conditions. LAURA employs a two-temperature and 18-species model at trajectory points prior to and including peak dynamic pressure, and it employs shock capturing. For these comparisons, the LAURA program used a simplified non-argon Martian atmosphere composition as input. The inflow boundary and grid were aligned with the captured bow shock, and species mass fractions were held fixed at their free-stream values. LAURA has been used to generate inviscid perfect gas solutions and to ascertain sensitivity for its solutions of aerodynamic coefficients at selected trajectory points [9].

Examples of runs of the LAURA program of Mars Pathfinder at 50 seconds and 60 seconds past entry are presented. Figure 6 displays electron-density contours in the wake region for the 50-seconds past entry point. Figure 7 displays electron-density contours in the wake region for the 60-seconds past entry point. The LAURA software factors the shape of the spacecraft vehicle but does not consider ablation products from the vehicle itself, which are assumed negligible. The SLA-561 thermal protection system is considered partially ablative, but is not expected to contribute significantly to the charged particles at the high velocities encountered during the entry period.

For the case at 50 seconds past entry (a shock velocity of 7.4 km/s and an altitude of 56 km), the Horton program estimated a stagnation electron density of $n_e = 1.2 \times 10^{14}/\text{cm}^3$ versus the LAURA estimate of $6.3 \times 10^{13}/\text{cm}^3$. The wake-region electron number density was approximated from the Horton stagnation point electron number density to be $n_e = 1.1 \times 10^{12}/\text{cm}^3$ using Eq. (16). The contour curves of the LAURA program run for the same case show electron densities as high as $\sim 10^{12}/\text{cm}^3$ (see Fig. 6) in the wake region and in excess of the critical electron density, $\log(n_e) \sim 11.94$, at the expected BLGA antenna aspect angle[8] ($\simeq 6$ deg). The signal blackout period started at 49 seconds past entry.

[7] E. Satorius, op cit.

[8] D. Spencer and R. Cook, *Mars Pathfinder Project Trajectory Characteristics Document Preliminary Version,* JPL D-10935, Rev. A (internal document), Jet Propulsion Laboratory, Pasadena, California, December 1, 1994.

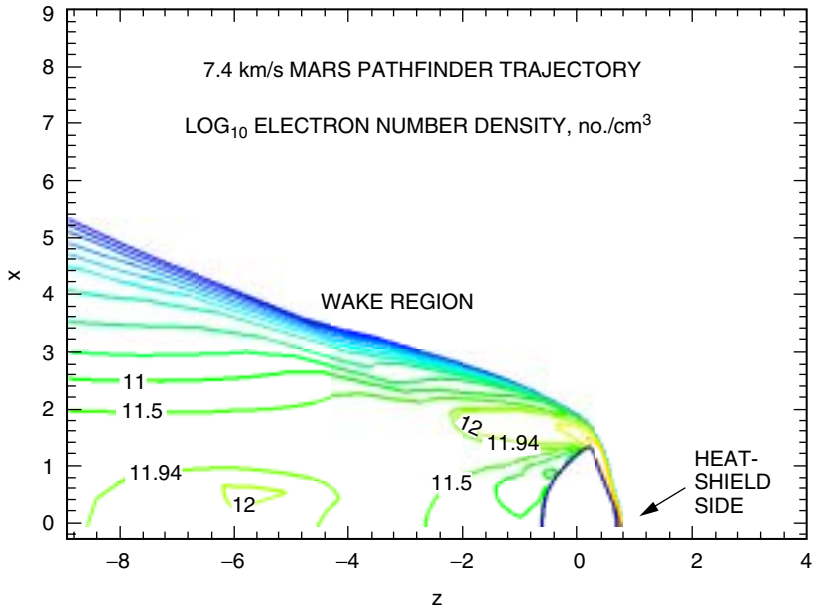

Fig. 6. Mars Pathfinder Langley Research Center wake region electron density contours at 50 s past entry. (Courtesy of Peter Gnoffo.)

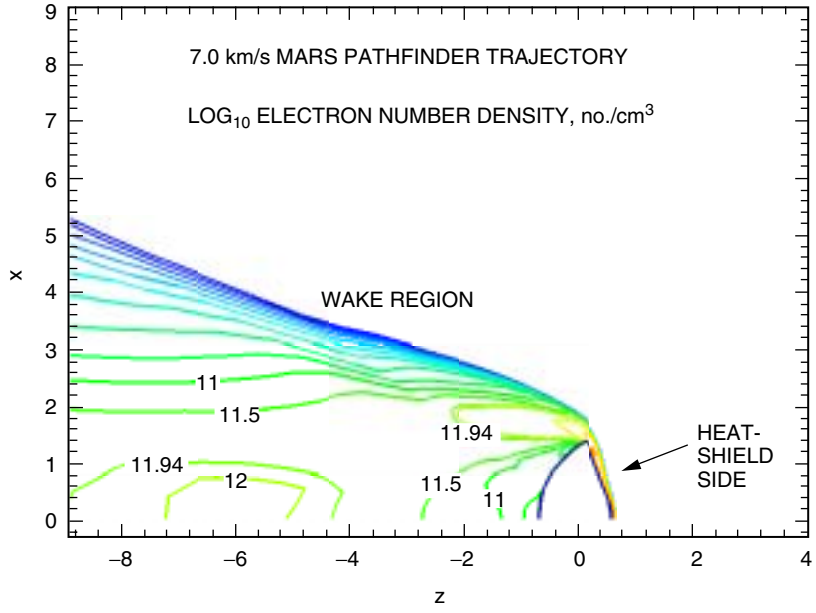

Fig. 7. Mars Pathfinder Langley Research Center wake region electron density contours at 60 s past entry. (Courtesy of Peter Gnoffo.)

The two programs also were compared at 60 seconds past entry (a shock velocity of 7 km/s and an altitude of 48 km). The Horton program estimated a stagnation electron number density of $n_e = 1.7 \times 10^{14}/\text{cm}^3$ versus the LAURA estimate of $6.3 \times 10^{13}/\text{cm}^3$. The Horton program wake-region electron number density estimate was $n_e = 1.7 \times 10^{12}/\text{cm}^3$ using Eq. (16). The results of the LAURA program contour plot output show electron densities as high as $n_e \sim 10^{12}/\text{cm}^3$ (see Fig. 7) and exceeding the critical electron density required for blackout at the expected BLGA aspect angle[9] ($\simeq 6$ deg). Both the

[9] D. Spencer and R. Cook, ibid.

JPL Horton and the Langley Research Center LAURA programs estimate wake-region electron densities, which exceed the critical electron density for an X-band communications blackout at 50 seconds and 60 seconds past entry, consistent with the observed blackout.

The LAURA program estimates for the stagnation point electron number densities lie below the Horton estimates, as expected. The algorithm used in the Horton program assumes equilibrium conditions, while the LAURA program was run in a non-equilibrium mode, which allows for recombining (factoring in the transit time considerations). The Horton estimates thus are considered to be conservative and serve as an upper bound to the electron density. The wake-region electron-density approximation of Eq. (16) is to be treated with caution as there is uncertainty associated with values of γ and κ changing during the entry profile. To minimize this uncertainty, a value of $\kappa = 3.5$, determined from stagnation and wake-region estimates run by LAURA, was employed to more accurately reflect the pressure ratio across the shock from the stagnation point to the wake region. This served as a reasonable calibration at 50 seconds and 60 seconds past entry, where the Horton wake-region estimates are in reasonable agreement with the LAURA wake-region electron number density estimates. For several other data points where both programs do not predict blackout, there are larger discrepancies between the estimates output from the two programs.

VII. Predictions for Mars Exploration Rover

The Mars Exploration Rovers (MER-A and MER-B) are expected to be launched around May–June 2003 and to enter the Martian atmosphere in January 2004. MER will perform a variety of scientific experiments using rovers, which will be outfitted with X-band direct to Earth communications and UHF proximity links.

The X-band link to Earth will use semaphores to monitor status of the spacecraft during the entry-descent-landing (EDL) phase. The MER spacecraft will enter the Martian atmosphere at a much lower velocity (5.5 km/s) than did Mars Pathfinder (7.6 km/s). The levels of electron densities for MER's atmospheric entry therefore are expected to be significantly lower than those of Mars Pathfinder. MER will enter with an entry angle of -12 deg, a nominal angle of attack of $\alpha \sim 0$ deg, and will use a spin-stabilized guidance and control system.

Since MER-B will enter the Martian atmosphere at a slightly higher velocity than MER-A, only the MER-B case will be examined and will serve as a bound for both spacecraft. The predicted MER-B baseline trajectory of velocity versus time past entry is shown in Fig. 8(a) and that of altitude versus time past entry in Fig. 8(b).[10] The stagnation point and wake-region electron-density profiles resulting from using the approach of Section IV are shown in Fig. 9. The Horton program runs used the modern-day no-argon simplification Mars atmosphere model as input.

The MER-B peak heating rate is expected to be maximum at about 102 seconds after entry, at a velocity of 4.9 km/s and at an altitude of 42.6 km. The peak dynamic pressure is expected to occur at 118 seconds past entry.

The stagnation electron-density predicted from the program at 102 seconds past entry is $\sim 1.7 \times 10^{10}/\text{cm}^3$. The predicted wake-region electron density at this time, using the approximation of Eq. (16), is $\sim 4 \times 10^8/\text{cm}^3$, which lies over three orders of magnitude below the critical X-band electron density of $8.8 \times 10^{11}/\text{cm}^3$ (see Table 1) required for blackout. Thus, based on this example test point and other data points as plotted in Fig. 9, MER is not predicted to experience a communications blackout due to charged particles during its entry and descent into the Martian atmosphere. A LAURA program run at 100 seconds past entry results in an electron density, which supports this prediction that blackout due to shock-induced charged particles is unlikely for MER.

[10] The trajectory was provided by P. Desai, Jet Propulsion Laboratory, Pasadena, California, August 13, 2001.

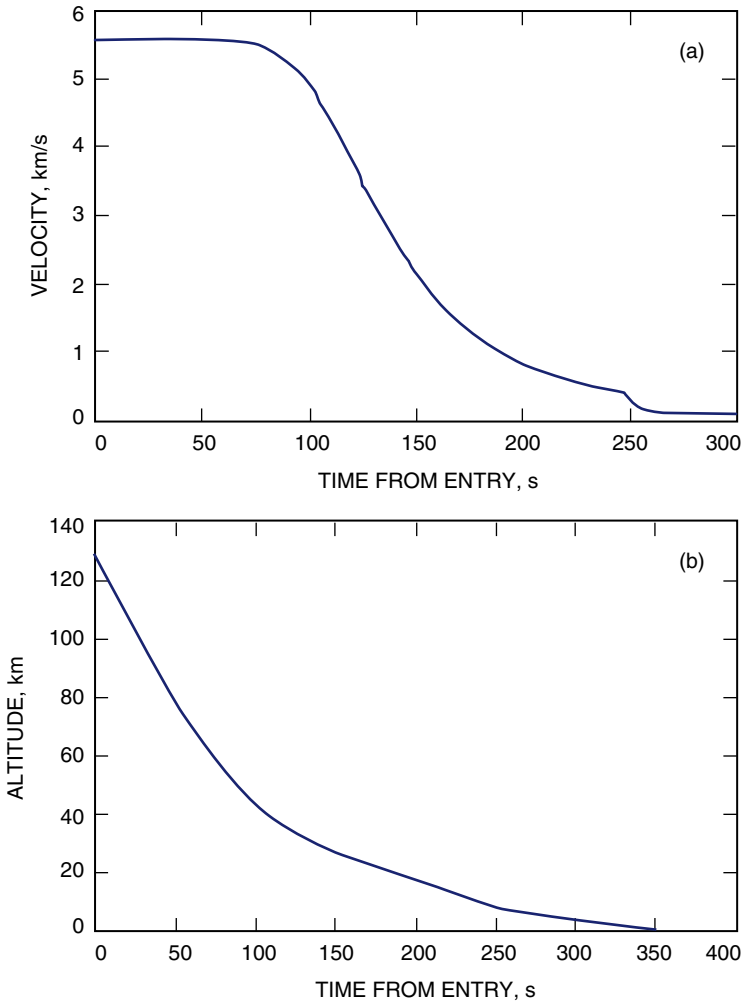

Fig. 8. MER-B entry velocity and altitude profiles: (a) entry velocity and (b) altitude.

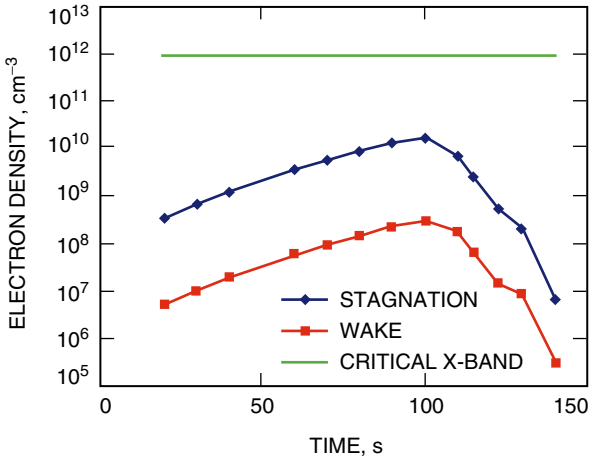

Fig. 9. MER-B predicted electron number density profiles.

VIII. Earth Entry Cases Studied

The Earth atmosphere model is about 78 percent N_2, 21 percent O_2, and 1 percent argon, referenced to sea level with a surface pressure of 1013 mb. The atmospheric scale height is about 7 km (see Table 2).

During the 1960s, NASA conducted several experiments involving Earth atmospheric entry studies in order to prepare for the Apollo missions. For Apollo, the interaction of the high-speed capsule with the Earth's atmosphere caused communications blackouts of several minutes at the S-band communications frequency [6]. The critical plasma density at S-band is $6.6 \times 10^{10}/\text{cm}^3$ (see Table 1). Although Apollo was highly ablative, pure-air chemistry dominated the generation of plasma at the high velocities [6].

A proposed aero-assist flight experiment [11] was to obtain data at several different frequencies using reflectometry sensors, which were to be used to validate the computational fluid dynamics (CFD) LAURA software [9]. Greendyke et al. [11] performed CFD predictions using LAURA and observed that the electron-density signature as a function of distance from the wall of the spacecraft includes a dual-plateau effect. The number of electrons generated would increase significantly, caused by the onset of electron impact ionization, which becomes an important mechanism once a critical electron density is reached. The Horton program was run for several velocity–altitude pairs provided in Greendyke et al. [11]. The resulting Horton-derived electron densities were compared against the peak electron densities in [11]. Good agreement was found of less than an order of magnitude. The Horton electron-density estimates were biased down about 23 percent with a 26 percent standard deviation, relative to the Greendyke et al. [11] electron densities.

The Horton program was run for known velocity–altitude boundaries of predicted and measured blackout data from the Apollo program. The blackout boundaries were derived from Cornell Aerodynamic Laboratory predictions for pure air, which neglect ablation products affecting impurity ionization [6]. Dunn [6] compared these predictions with actual in-flight data gathered by NASA from Apollos 4, 6, 7, 8, and 10 and found very good agreement. Wake-region electron densities for the blackout boundaries in [6] were estimated from the Horton stagnation densities, using the procedure outlined in Section IV. These electron densities were compared with the critical S-band electron density of $6.6 \times 10^{10}/\text{cm}^3$ and are plotted in Fig. 10. The estimates agree well with the critical S-band density at the 50 percent level for altitudes below 90 km. However, for altitudes above 90 km, the Horton estimates were a factor of five high in this region, which is in the non-equilibrium realm, where Dunn [6] employed a different formulation. A

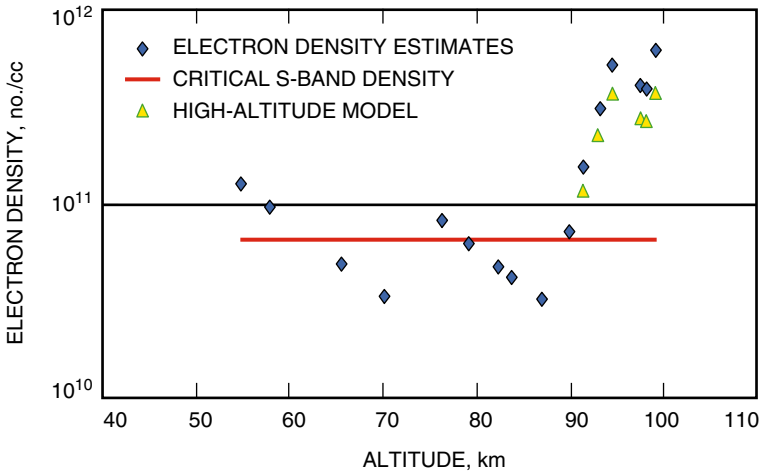

Fig. 10. Horton program wake region electron density estimates versus altitude at Apollo blackout boundary.

viscous-flow analysis for an Apollo-type vehicle is applicable for these higher altitudes (76 km to 122 km), which assumes free molecular flow conditions. The equilibrium-constrained Horton program produces an overestimation of electron densities under non-equilibrium conditions, and this result illustrates this point.

For altitudes below 86 km, a continuum thin boundary layer is assumed, and the atmosphere is homogeneously mixed with a relative volume composition leading to a constant mean molecular weight. The air is treated as a perfect gas, and the pressure temperature and density at any point can be related by an equation of state. The atmosphere is in a state of hydrostatic equilibrium and horizontally stratified. For altitudes above 86 km, the hydrostatic equilibrium of the atmosphere starts to break down, leading to the need for a different model [12]. Molecular oxygen dissociation becomes significant above 85 km, and diffusive separation becomes significant at about 100 km [12]. The effect of vertical winds also becomes important [12].

The Horton program was rerun for Apollo blackout profile points above 90 km, adjusting for the initial composition and density based on the values provided in the tables of [12]. By taking into account the composition of the atmosphere above 90 km (dissociation of O_2) and a different pressure dependence with temperature at these altitudes, the resulting Horton electron-density estimates were reduced (see Fig. 10) but were still higher than the critical blackout density by a factor of 2.7. Further revision of the Horton program to more accurately handle high-altitude profile points or to employ correction factors is the subject of further work. The Horton estimates for altitudes below 90 km are believed to be accurate to 50 percent, a reasonable level to test for likelihood of blackout.

A proposed Earth aero-capture demonstration atmospheric passage profile[11] was examined to test whether or not a blackout would occur at S-band, X-band, and 32 GHz (Ka-band). The velocity–altitude profile of the proposed aero-capture experiment at the worst-case bank angle expected to produce the longest blackout period was input to the Horton program using the nominal Earth atmosphere model. The predicted stagnation point and wake-region density profiles for this profile are shown in Fig. 11, along with a spot check (Langley Research Center) using the LAURA program.[12] The LAURA profile data point assumed a fore-body 0-degree angle of attack, 11 species, the 2-temperature model, at a velocity of $V = 9.5$km/s and an altitude of 75 km. The resulting LAURA stagnation electron density of $2.86 \times 10^{14}/\text{cm}^3$ and wake-region density of $2 \times 10^{12}/\text{cm}^3$ [using the approximation of Eq. (16)] both exceed the critical S-band electron density ($6.6 \times 10^{10}/\text{cm}^3$) required for blackout. Upon examination of Fig. 11, the expected blackout period would be about 280 seconds for S-band and 130 seconds for X-band. Using Ka-band, there would be no blackout. As these estimates have order-of-magnitude uncertainties assigned to them, the range of expected blackout periods at each frequency can be deduced by moving the wake-region curve up and down as appropriate.

IX. Conclusion

A description of the Horton aero-thermodynamic tool was provided, for which the intended use is to predict wake-region electron-density profiles of atmospheric entry of spacecraft to assess whether or not a communications blackout condition will occur.

Based on wake-region electron-density estimates produced by the Horton program, the Mars Pathfinder communications blackout at X-band may possibly be attributed to a charged-particle sheath created by shock-induced thermal heating, which occurred during entry into the Martian atmosphere. The estimated wake-region electron densities exceeded the critical X-band plasma density required for a communications blackout during the first 20 seconds of the 30-second blackout period. Independent checks using the

[11] G. Barton, *ST-7 Aerobraking Trajectories,* Draper Laboratory, Cambridge, Massachusetts, October 9, 2001.

[12] N. Cheatwood, personal communication, Langley Research Center, Hampton, Virginia, October 25, 2001.

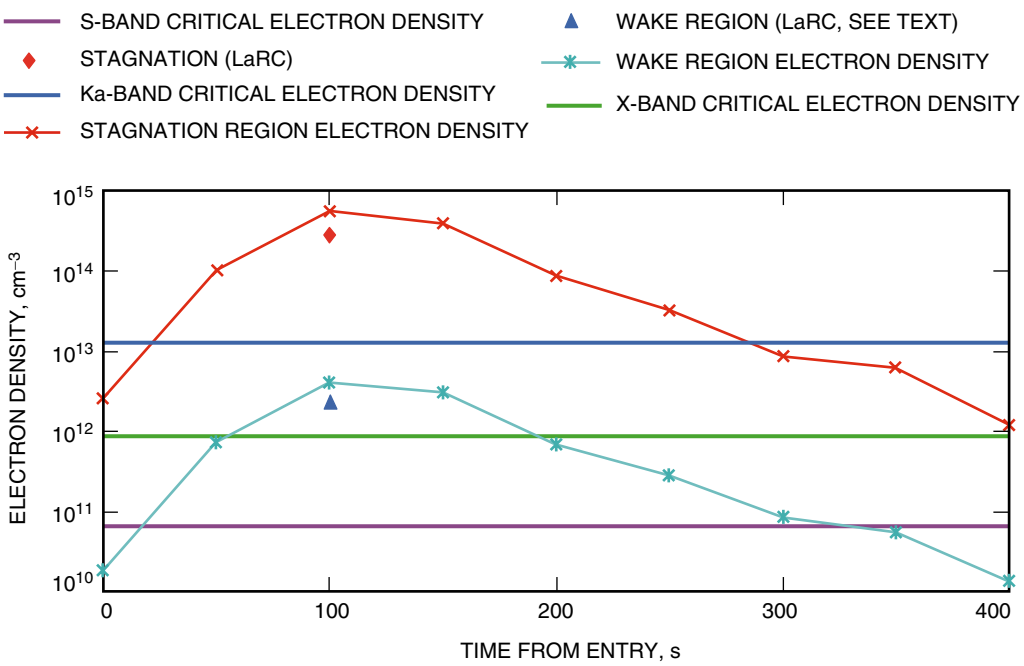

Fig. 11. Proposed Earth aero-capture mission predicted electron number density profiles and critical electron number densities.

Langley Research Center LAURA program concur with this result. Combinations of other factors, such as high Doppler rates and low SNR, may have contributed to the outage during the last few seconds.

The upcoming MER missions are not expected to undergo communications blackout due to charged particles during their EDL phases as their wake-region electron densities are predicted to lie more than three orders of magnitude below the critical X-band plasma density.

Several cases dealing with Earth entry also have been studied. The Horton program displayed good agreement to the 50 percent level with Apollo blackout boundaries for altitudes below 86 km, in the expected equilibrium realm.

Possible future work includes revising the Horton program with upgrades to accommodate finer temperature resolution (100 K instead of 500 K), to accommodate corrections under non-equilibrium conditions, and to generate curves of electron density versus altitude and atmosphere relative velocity using the modern-day Mars atmosphere model. These curves can be useful to future missions in order to assess whether a blackout condition will occur, and, if so, what the expected outage period will be in order to factor it into their operational scenarios. The program also can be used to assess blackout conditions for entry into atmospheres of other planetary bodies.

Acknowledgments

I would like to thank Chad Edwards and David Bell for their support of this study; Peter Gnoffo, Peter Ilott, Robert Mitchelltree, Vince Anicich, Ed Satorius, and Christian Ho for many informative discussions; Peter Gnoffo of Langley Research Center for running the LAURA (Langley Aero-thermodynamic Upwind Relaxation Algorithm) software to provide independent checks of the Mars entry cases and also providing electron density contour plots; Neil Cheatwood for running the LAURA software to provide checks for Earth entry cases; Ed Satorius for providing details on the FFT analysis of the Mars Pathfinder open-loop data acquired during atmospheric entry; Diana Parseghian for assistance in recovering the Horton program code and the supporting data files; and, finally, Polly Estabrook for her comments and very much appreciated support of and enthusiasm for this endeavor.

References

[1] G. E. Wood, S. W. Asmar, T. A. Rebold, and R. A. Lee, "Mars Pathfinder Entry, Descent, and Landing Communications," *The Telecommunications and Data Acquisition Progress Report 42-131, July–September 1997*, Jet Propulsion Laboratory, Pasadena, California, pp. 1–19, November 15, 1997. http://tmo.jpl.nasa.gov/tmo/progress_report/42-131/131I.pdf

[2] T. E. Horton, *The JPL Thermochemistry and Normal Shock Computer Program,* JPL Technical Report 32-660, Jet Propulsion Laboratory, Pasadena, California, November 1, 1964.

[3] J. D. Nordgard, "A Martian Entry Propagation Study," *Radio Science,* vol. 11, no. 11, pp. 947–957, November 1976.

[4] D. Spencer, *An Evaluation of the Communication Blackout Problem for a Blunt Mars-Entry Capsule and a Potential Method for the Elimination of Blackout,* JPL Technical Report 32-594, Jet Propulsion Laboratory, Pasadena, California, April 15, 1964.

[5] E. A. Brummer, "X-band Telemetry Systems for Re-Entry Research," L-3521, presented at the IEEE Region 3 Meeting, Richmond, Virginia, April 24–26, 1963.

[6] M. G. Dunn, "Comparison Between Predicted and Measured Blackout Boundaries for Earth Entry of Apollo," NASA Technical Report 71N21104, January 1970.

[7] C. Park, J. T. Howe, R. L. Jaffe, and G. V. Chander, "Revision of Chemical-Kinetic Problems of Future NASA Missions, II: Mars Entries," *Journal of Thermophysics and Heat Transfer,* vol. 8, no. 1, January–March 1994.

[8] P. A., Gnoffo, R. N. Gupta, and J. L., Shinn, "Conservation Equations and Physical Models for Hypersonic Air Flows In Thermal and Chemical Non-equilibrium," NASA Technical Paper 2867, National Aeronautics and Space Administration, 1989.

[9] P. Gnoffo, J. Weilmuenster, R. Braun, and C. Cruz, "Effects of Sonic Line Transition on Aerothermodynamics of the Mars Pathfinder Probe," AIAA 95-1825, 13th AIAA Applied Aerodynamics Conference, San Diego, California, p. 14, June 19–22, 1995.

[10] D. A. Spencer, R. C. Blanchard, R. D. Braun, P. H. Kallemeyn, and S. W., Thurman, "Mars Pathfinder Entry, Descent, and Landing Reconstruction," *Journal of Spacecraft and Rockets,* vol. 36, no. 3, pp. 357–366, May–June 1999.

[11] R. Greendyke, P. Gnoffo, and R. Lawrence, "Calculated Electron Number Density Profiles from the Aeroassist Flight Experiment," *Journal of Spacecraft and Rockets,* vol. 29, no. 5, pp. 621–626, September–October 1992.

[12] National Oceanic and Atmospheric Administration, NASA, and U.S. Air Force, *U.S. Standard Atmosphere, 1976,* NOAA-S/T 76-1562, Washington D.C., October 1976.